



Detection of Intact Vancomycin-Arginine as the Active Antibacterial Conjugate in *E. coli* by Whole Cell Solid-State NMR

Journal:	<i>RSC Medicinal Chemistry</i>
Manuscript ID	MD-RES-04-2023-000173.R1
Article Type:	Research Article
Date Submitted by the Author:	08-May-2023
Complete List of Authors:	Werby, Sabrina; Stanford University Brcic, Jasna; Stanford University Chosy, Madeline; Stanford University Sun, Jiuzhi; Stanford University Rendell, Jacob; SuperTrans Medical, Ltd Neville, Lewis; SuperTrans Medical, Ltd Wender, Paul; Stanford University Cegelski, Lynette; Stanford University,

ARTICLE

Detection of Intact Vancomycin-Arginine as the Active Antibacterial Conjugate in *E. coli* by Whole Cell Solid-State NMR

Received 00th January 20xx,
Accepted 00th January 20xx

Sabrina H. Werby¹, Jasna Brčić¹, Madeline B. Chosy¹, Jiuzhi Sun¹, Jacob T. Rendell², Lewis F. Neville², Paul A. Wender,^{1,3*} Lynette Cegelski^{1*}

DOI: 10.1039/x0xx00000x

The introduction of new and improved antibacterial agents based on facile synthetic modifications of existing antibiotics represents a promising strategy to deliver urgently needed antibacterial candidates to treat multi-drug resistant bacterial infections. Using this strategy, vancomycin was transformed into a highly active agent against antibiotic-resistant Gram-negative organisms *in vitro* and *in vivo* through the addition of a single arginine to yield vancomycin-arginine (V-R). Here, we report detection of the accumulation of V-R in *E. coli* by whole cell solid-state NMR using ¹⁵N-labeled V-R. ¹⁵N CPMAS NMR revealed that the conjugate remained fully amidated without loss of arginine, demonstrating that intact V-R represents the active antibacterial agent. Furthermore, C{N}REDOR NMR in whole cells with all carbons at natural abundance ¹³C levels exhibited the sensitivity and selectivity to detect the directly bonded ¹³C-¹⁵N pairs of V-R within *E. coli* cells. Thus, we also present an effective methodology to directly detect and evaluate active drug agents and their accumulation within bacteria without the need for potentially perturbative cell lysis and analysis protocols.

Introduction

We face a future where our current arsenal of antibiotics could be rendered ineffective by drug-resistant microbes. This is particularly alarming for highly prevalent bacterial infections such as complicated urinary tract infections (cUTI), associated with the highest “critical priority” Gram-negative pathogens as identified by the World Health Organization^{1,2}. There is an urgent need for the expeditious development of new antimicrobials in consort with novel interventions to combat antimicrobial resistance. Towards this end, we recently introduced new vancomycin conjugates effective against drug-resistant Gram-positive and Gram-negative ESKAPE pathogens. Vancomycin itself is a widely prescribed glycopeptide antibiotic reserved for the treatment of Gram-positive bacteria. It inhibits peptidoglycan biosynthesis required for cell-wall synthesis and cell viability by sequestering Lipid II peptidoglycan precursors at the exo-face of the cell membrane^{3,4}. In order to improve efficacy and overcome resistance, vancomycin has been extensively modified over the past three decades and several vancomycin analogs, including oritavancin, telavancin, and dalbavancin have been clinically approved for the treatment of Gram-positive infections. In contrast to previously reported semisynthetic or lipophilic derivatives, we introduced a compound consisting of vancomycin

linked by an aminohexanoic acid spacer to D-octaarginine (r8), resulting in the compound we termed V-r8⁵. The design of this conjugate was inspired by the cell-penetrating activity of guanidinium-rich molecular transporters including arginine-rich contiguous and spaced peptides, and guanidinium-rich peptoids and nonpeptidic agents^{6–10}, that deliver a variety of cargos, including antimicrobials^{11–15}, chemotherapeutics^{16,17}, peptides^{18–20}, proteins^{21,22}, inositol polyphosphates²³, and oligonucleotides (RNA, DNA)^{6,24–26} into cells *in vitro* and *in vivo*. We hypothesized that conjugates of vancomycin and octaarginine would exhibit improved penetration through biofilm barriers and enhanced cell association by engaging anionic cell-surface agents and potentially enhancing transport across the cell membrane. In line with our hypothesis, V-r8 exhibited significantly improved (4–128 fold) activity against Gram-positive organisms, including vancomycin-resistant enterococci⁵. Significantly, V-r8 outperformed vancomycin, often by orders of magnitude, in all persist cell and biofilm assays, and was superior to current clinically used agents in a murine biofilm infection model. Furthermore, we uncovered vancomycin conjugates with highly promising antibacterial activities towards Gram-negative bacteria^{27,28}.

Indeed, conjugates of vancomycin with a single amino acid, including that of vancomycin and a single arginine, termed V-R, were discovered to be effective at killing “critical priority” drug-resistant Gram-negative organisms²⁷. Unlike Gram-positive bacteria, *E. coli* and other Gram-negative pathogens contain a dual membrane architecture and contain a thin layer of peptidoglycan in the periplasm, surrounded by the outer membrane. Cell-wall targeting antibiotics must breach the outer membrane barrier in Gram-negative bacteria to access peptidoglycan precursors and

¹Department of Chemistry, Stanford University, Stanford, CA 94305, USA

²SuperTrans Medical Ltd., Ness Ziona, Israel

³Department of Chemical and Systems Biology, Stanford University, Stanford, CA 94305, USA

Corresponding Authors

*E-mail: wenderp@stanford.edu (P.A.W.).

*E-mail: cegelski@stanford.edu (L.C.).

the assembly machinery in the periplasm. Thus, although the binding sites for vancomycin are present in Gram negative pathogens, it is generally ineffective in killing Gram-negative bacteria at relevant concentrations. V-R presents an urgently needed new antibacterial candidate effective against all extended spectrum beta-lactamase (ESBL)-positive *E. coli*, including carbapenemase-containing *E. coli* and other Gram-negative bacteria, while retaining antibacterial activity against Gram-positive organisms²⁷. Mechanistically, V-R treatment resulted in inhibition of peptidoglycan synthesis and the accumulation of peptidoglycan precursors in *E. coli*²⁷. Thus, conjugation of vancomycin with arginine enables its association with and translocation across the outer membrane to access intracellular targets. This discovery simultaneously introduced V-R as a new molecular probe to study and evaluate cellular changes in Gram-negative bacteria due to vancomycin-like inhibition of peptidoglycan synthesis. V-r (the corresponding vancomycin-D-arginine conjugate) was selected for use in the first animal experiments, given the assumed enhanced stability of D-amino acid peptides and conjugates in mammalian hosts *in vivo*²⁸. Mammalian cell assays revealed that V-r exhibited no toxicity on human erythrocytes, HepG2 cells, and primary renal proximal tubule epithelial cells. V-r was characterized by a lower frequency-of-resistance than ciprofloxacin (the standard-of-care therapy) and was superior in causing resolution of *E. coli* infection in a murine thigh muscle model as compared to ciprofloxacin²⁸. More recently, V-r demonstrated significant efficacy at low doses in a murine complicated urinary tract infection model as evaluated through bacterial burden in bladder, kidneys and urine²⁹. The estimated putative humanized dose was proposed to be potentially as low as 1-5 mg/kg²⁹. There is a high risk for long-term nephrotoxicity associated with vancomycin use and the use of many antibiotics for serious Gram-positive infections. Thus, the high concentrations of V-r available in the urinary tract, the relevant site for treating urinary tract infection, are highly favorable towards the desire to minimize doses and mitigate possible toxicity²⁹. Thus, single amino acid conjugates of vancomycin present an outstanding opportunity for further preclinical evaluations towards the clinical entry of vancomycin analogs to target Gram-negative bacteria^{27,28}. Additional vancomycin conjugates with activity against Gram-negative bacteria have been reported by others since our reporting of V-r8 and V-R. These include a lipophilic cationic vancomycin derivative³⁰, vancomycin with a C terminus guanidinium group modification³¹, additions of trimethylammonium salt modifications to both the C terminus³² and A ring³³ of vancomycin, and conjugation of polycationic peptides through a chemical linker to the N terminus, C terminus, A-ring, and vancosamine of vancomycin^{34,35}. Vancomycin with lipophilically acylated peptide sequences have also been designed to enhance vancomycin association and interactions with the cell membrane.

From antimicrobials to anticancer agents to the delivery of mRNA into cells, many innovative design strategies have been introduced to enhance drug delivery into cells and to enhance tissue and cell-selective delivery and uptake^{6,35}. In addition, remarkable design strategies have been employed in pro-drug approaches, wherein

the active drug payout and biodistribution is controlled by release from its covalently or non-covalently associated partnering molecule to improve efficacy and offer an expanded therapeutic window³⁶⁻³⁸. The determination of the active drug agent in drug conjugates or drug formulations is important in understanding drug mode(s) of action and for regulatory considerations towards human clinical studies of a new therapeutic candidate³⁹. We sought to determine whether V-R was the active agent responsible for killing *E. coli* or whether it was possible that free vancomycin was liberated from V-R once internalized in *E. coli*. We hypothesized that V-R is active as an intact conjugate given the direct conjugation of arginine to the bulky glycopeptide through an amide bond that would likely be less susceptible to enzymatic or chemical hydrolysis as compared to longer peptide scaffolds. Yet, bacteria harbor several amidases, particularly important in the cleavage of peptidoglycan during cell wall remodeling and division⁴⁰. In recent animal model experiments the use of V-r (using D-arginine) was motivated by the generally enhanced stability of D-amino acid peptides and conjugates in mammalian hosts *in vivo*, however the stability of V-R or V-r as it operates in bacteria was not evaluated.

Here, we designed a whole cell solid-state NMR approach to directly detect the accumulation of V-R in intact *E. coli* cells and to determine whether the conjugate was intact or whether arginine was liberated from the conjugate during conditions in which V-R kills *E. coli*. Solid-state NMR is uniquely suited to detect specifically labeled nuclei and specific single bonds in the context of bacterial, plant and mammalian whole cells, intact plant leaves and mammalian tissues and can be used holistically to profile all carbon and nitrogen contributions in cells with dozens of publications with some referenced here with most relevance for this study.⁴¹⁻⁴⁴ Whole-cell NMR studies delivered parameters of cell-wall composition and antibiotic-cell wall binding sites to more completely define the influence of vancomycin and oritavancin in Gram-positive *S. aureus* and enterococci⁴⁵⁻⁵⁵ and to characterize antimicrobial peptide influences on membrane lipids in *E. coli*⁵⁶⁻⁵⁸.

Results and discussion

In this study, a selectively isotopically labeled V-R was synthesized to permit detection of V-R in *E. coli*. V-R was synthesized using L-[¹⁵N₄]arginine in order to introduce ¹⁵N that would be incorporated into the moiety directly bonded to the vancomycin C-terminus and thus report as an amide nitrogen (Figure 1A). If the L-[¹⁵N₄]arginine or other designed moiety would be liberated from vancomycin, the amide nitrogen chemical shift would convert to that of an amine nitrogen. Furthermore, we hypothesized that C{N}Rotational-echo Double Resonance (REDOR) NMR would exhibit the sensitivity and enable us to detect V-R directly in cells by selecting the V-R carbons that are present at natural abundance ¹³C levels through one-bond dipolar couplings to the selectively introduced ¹⁵N atoms in the molecule, even amidst all the cellular carbons also present at natural abundance.

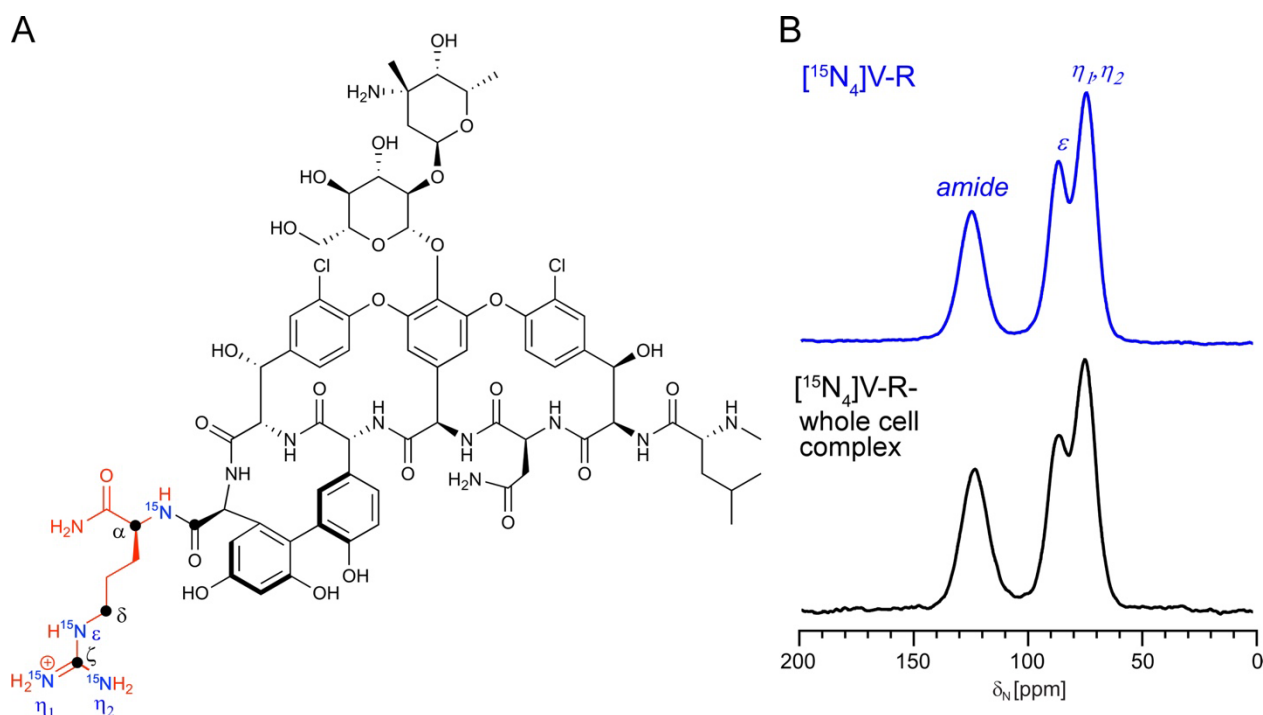


Figure 1. Chemical structure of $[^{15}\text{N}_4]\text{V-R}$ and detection of V-R amide nitrogens in the whole cell complex. (A) Vancomycin (black) is chemically conjugated through an amide bond to L-arginine (red) containing four ^{15}N labeled nitrogen atoms (blue). Carbons directly bonded to ^{15}N are shown with solid black circles. (B) ^{15}N CPMAS of pure $[^{15}\text{N}_4]\text{V-R}$ and $[^{15}\text{N}_4]\text{V-R}$ treated *E. coli*. Spectra of the pure antibiotic (blue) and V-R associated with treated whole cells (black) show intensity exclusively in the amide region. Each spectrum was the result of 32,768 scans and recycle delay of 2 s.

The *E. coli* reference strain ATCC 25922 was selected for our whole cell NMR analysis due to its broad inclusion in many antibacterial activity studies, permitting broadly applicable comparative data for future studies by others. The MIC of V-R against *E. coli* 25922 is $8\ \mu\text{M}$ ²⁸. The MIC corresponds to the lowest concentration of compound sufficient to inhibit growth of bacteria in a defined time period in which the given concentration of antibiotic is added to a cell culture with a bacterial density of approximately 5×10^5 cells/mL. Higher concentrations of antibiotic are required for higher density cell cultures⁵⁹. For preparation of a whole cell sample of approximately 20 mg, *E. coli* were grown in 150 mL Mueller Hinton nutrient broth to exponential phase with an OD_{600} of 0.6, corresponding to 2×10^8 cells/mL as determined by broth dilution and plating. Bacteria were then collected by centrifugation after reaching the optical density (OD_{600}) of 0.6 and resuspended in 10 mL of 5 mM glucose/5 mM HEPES containing 6 mg of $[^{15}\text{N}_4]\text{V-R}$. An MIC of $8\ \mu\text{M}$ is effective in preventing growth of $\sim 5 \times 10^5$ cells/mL. Thus, an approximate corresponding concentration of antibiotic to kill $\sim 2 \times 10^8$ cells/mL would be $400\ \mu\text{M}$. The 6 mg of V-R treatment with cells in a 10 mL volume corresponds to $370\ \mu\text{M}$. Cells were treated for 15 min and the whole cell-antibiotic complexes were collected by centrifugation with removal of excess buffer and free compound in solution. Using these conditions, bacteria were killed and unable to grow following introduction into fresh medium (no increase in OD_{600}), whereas bacteria from untreated control samples continued to divide and multiply from the OD of 0.6 to approximately OD 2.0 after 2 hours. The V-R-treated whole cell pellet was flash frozen in liquid nitrogen and lyophilized. The dry

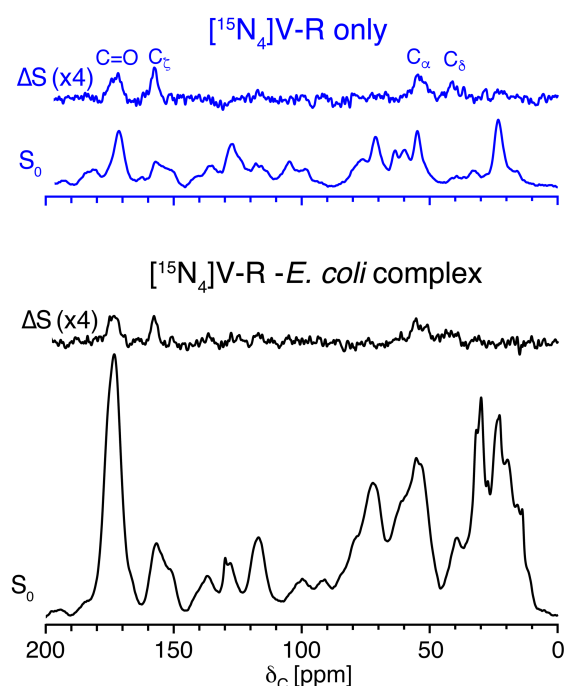


Figure 2. $\text{C}\{^{15}\text{N}\}$ REDOR of $[^{15}\text{N}_4]\text{V-R}$ (7 mg) and the $[^{15}\text{N}_4]\text{V-R}$ -*E. coli* complex (18 mg). $\text{C}\{^{15}\text{N}\}$ REDOR with a 2.2 ms REDOR evolution time identified carbons directly bonded to ^{15}N in $[^{15}\text{N}_4]\text{V-R}$ (top, blue spectra). These carbons are also detected in the $[^{15}\text{N}_4]\text{V-R-E. coli}$ cell complex (bottom, black spectra). Each REDOR S_0 and S spectrum was the result of 110,592 scans.

mass of the resulting whole cell-V-R complex was 25 mg of which 18 mg was transferred to a thin-wall (36 μ L capacity) 3.2 mm outer diameter zirconia rotor. The whole cell complex as well as the pure compound, [$^{15}\text{N}_4$]V-R, were analyzed by ^{15}N cross-polarization magic-angle spinning (CPMAS)⁶⁰ and C{N}REDOR NMR⁶¹. The arginine N-terminus nitrogen is directly bonded to vancomycin and displays the amide chemical shift centered at 123 ppm. The two terminal guanidinium nitrogens (η_1 , η_2) appear at 74 ppm and the ϵ -nitrogen closer to the backbone is centered at 86 ppm. The ^{15}N CPMAS analysis of the whole cell complex yielded excellent sensitivity, with detection of the nitrogens in [$^{15}\text{N}_4$]V-R. Most notably, there is no appearance of an amine peak (Figure 1B, bottom spectrum). Thus, arginine has not been liberated from vancomycin. The ^{15}N CPMAS detection of [$^{15}\text{N}_4$]V-R-treated *E. coli* revealed that intact V-R is the active antibacterial agent.

To further interrogate the whole cell complex, we extended the solid-state NMR approach to observe all the carbons at natural abundance ^{13}C levels in the V-R-whole cell complex. Whole cell CPMAS NMR experiments using natural abundance ^{13}C detection have previously been directed to detect carbon compositional pools of different *E. coli* strains as well *E. coli* ribosomes^{41,62}. Here, we performed a C{N}REDOR measurement to select and identify carbons directly bonded to a labeled nitrogen (Figure 2). The REDOR experiment is performed in two parts. A full-echo reference (S_0) spectrum contains all the carbon contributions in the whole cell-V-R complex. A dephased (S) spectrum is obtained in a separate spectral acquisition, in which we restore ^{13}C - ^{15}N dipolar couplings that are suppressed by magic-angle spinning (MAS) using π pulses. Thus, the REDOR difference (ΔS) spectrum provides the full set of carbons within a certain distance of nitrogen, depending on the evolution time allowed for recoupling. We employed a 2.24 ms evolution time (16-Tr with 140 μ s rotor period corresponding to 7143 Hz MAS) to select and dephase all carbons directly bonded to nitrogen (C-N pairs with strong dipolar couplings of ~ 900 Hz, corresponding to ~ 1.5 \AA). These carbons are represented in the chemical structure of V-R with solid black circles (Fig. 1A). The ΔS spectrum revealed the carbons with chemical shifts directly corresponding to the anticipated carbons bonded to nitrogen in V-R (Figure 2). Furthermore, C{N}REDOR on the pure V-R compound yielded a similar ΔS spectrum (Figure 2, top). Specifically, we observed dephasing of carbons at 173 ppm, corresponding to the vancomycin C-terminal carbonyl conjugated to the arginine N-terminus. This provides additional direct evidence that the vancomycin-arginine amide bond remains intact after treatment of *E. coli* with V-R. As anticipated, dephasing by ^{15}N is also observed for the arginine α -carbon (C_2) at 56 ppm, the C_8 carbon at 42 ppm, and the terminal guanidinium carbon (C_c) at 158 ppm (Figure 2).

Conclusions

Drug conjugates can be metabolized in cells through chemical and enzymatic hydrolysis and, in the case of bacteria, specifically through cell wall remodeling amidases. Owing to the extraordinary activity of V-R as an active agent against Gram-negative bacteria, including uropathogenic *E. coli*, it was pressing to reveal whether V-R or liberated vancomycin without arginine

is the active agent within *E. coli* to inhibit peptidoglycan synthesis. We determined that the intact V-R conjugate is the active agent and is not operating in *E. coli* through a pro-drug mechanism wherein arginine is liberated from V-R or otherwise chemically modified. The ^{15}N CPMAS analysis is a direct way to identify and distinguish between amide and amine nitrogen contributions in whole cell samples and enabled this determination. Here, we additionally highlighted the power of utilizing C{N}REDOR with carbons at natural abundance, to obtain single bond selections to detect drug carbons in the context of whole cell samples. This approach is applicable to other antibiotics and antimicrobial conjugates as well as prodrugs that are designed for release of an active agent.

Experimental

Synthesis and characterization of [$^{15}\text{N}_4$]V-R.

[$^{15}\text{N}_4$]V-R was synthesized by WuXi AppTec (Shanghai, China) from commercially available vancomycin HCl (StruChem, Wujiang City, China, batch no. 20200412) and L-[$^{15}\text{N}_4$]arginine (Sigma-Aldrich, batch no. MBBC6301) according to the following procedure:

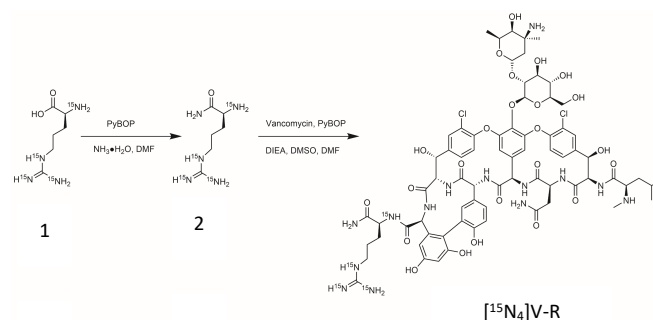


Figure 3. Synthesis of [$^{15}\text{N}_4$]V-R.

To a solution of compound 1 (60.0 mg, 347 μ mol) in DMF (2.00 mL) and $\text{NH}_3 \cdot \text{H}_2\text{O}$ (2.00 mL) was added PyBOP (233 mg, 448 μ mol). The reaction mixture was stirred at 25 $^\circ\text{C}$ for 18 hrs. LC-MS indicated that most of the reactant was consumed and desired product mass was detected. The reaction was concentrated under reduced pressure to remove solvent to afford compound 2 (300 mg, crude) as a colorless oil.

To a solution of **vancomycin** (344 mg, 237 μ mol) in DMF (3.00 mL) and DMSO (3.00 mL) was added PyBOP (264 mg, 508 μ mol), compound 2 (300 mg, crude) and DIEA (131 mg, 1.02 mmol). The resulting mixture was stirred at 25 $^\circ\text{C}$ for 12 hrs. LC-MS indicated that the starting material compound 2 was completely consumed and desired product mass was detected. The reaction mixture was filtered and the filtrate was purified by preparatory high-performance liquid chromatography to afford the TFA salt of [$^{15}\text{N}_4$]V-R (6.3 mg, 1.14% yield, 95% purity) as a white solid. Above-described procedure was repeated twice to yield a total of 17.2 mg material. The identity of the product was confirmed by mass spectrometry, with data as follows:

HRMS (ES+, m/z) calculated for C₇₂H₉₁Cl₂N₁₀O₂₄(¹⁵N)₄ (3+): 536.5191; Found: 536.5198.

HRMS (ES+, m/z) calculated for C₇₂H₉₀Cl₂N₁₀O₂₄(¹⁵N)₄ (2+): 804.2750; Found: 804.2760.

HRMS data are consistent with published HRMS data for the 3+ ion of unlabeled V-R: (ES+, m/z) calculated for C₇₂H₉₁O₂₄N₁₄Cl₂₃⁺: 535.1897, Found: 535.1905.²⁷

Whole cell-[¹⁵N₄]V-R sample preparation.

E. coli strain 25922 is a standard quality control strain and was obtained from the American Type Culture Collection (ATCC 25922). *E. coli* 25922 was grown in 150 mL Mueller Hinton nutrient broth to exponential phase (OD₆₀₀ = 0.6), corresponding to 2 × 10⁸ cells/mL as determined by broth dilution and plating. Bacteria were collected by centrifugation, resuspended in 10 mL of 5 mM glucose/5 mM HEPES containing 6 mg of [¹⁵N₄]V-R, and incubated at room temperature for 15 min. The whole cell-antibiotic complexes were collected by centrifugation with removal of excess buffer and free compound in solution. Using these conditions, bacteria were killed and unable to grow following introduction into fresh medium (observing no increase in OD₆₀₀), whereas bacteria from untreated control samples continued to divide and multiply from the OD₆₀₀ of 0.6 to approximately OD₆₀₀ 2.0 after 2 hours. The V-R-treated whole cell pellet was flash frozen in liquid nitrogen and lyophilized for solid-state NMR analysis.

Solid-state NMR spectroscopy experiments.

Experiments were performed in an 11.7 T wide-bore magnet (Agilent Technologies, Danbury CT) using an HCN BioMAS 3.2 mm Agilent probe (Agilent Technologies) with a DD2 console (Agilent Technologies). Samples were spun at room temperature in thin-wall (36 µL capacity) 3.2 mm outer diameter zirconia rotors at 7143 ± 2 Hz. CPMAS⁴⁷ was performed using ramped CP (1.5 ms) and with TPPM decoupling of ¹H at 92 kHz and a recycle delay of 2 s. Field strengths for ¹³C and ¹⁵N cross-polarization were all 50 kHz with π -pulses of 10 µs and with a 10% linear ¹H ramp centered at 57 kHz. TPPM ¹H decoupling was performed at 92 kHz during acquisition. 80 Hz exponential line broadening was applied to all free induction decays prior to Fourier transformation. Spectrometer chemical shift referencing was performed using ¹³C referenced to solid adamantane at 38.5 ppm.⁵²

Rotational-echo Double-resonance (REDOR) NMR⁴⁸ was used to restore the ¹³C-¹⁵N dipolar couplings that are removed by magic-angle spinning (MAS). REDOR experiments are performed in two parts, once with dephasing (S) and once without (full echo, S₀). The difference in signal intensity, referred to as the REDOR difference, ΔS (S₀ - S), for the observed spin is directly related to the corresponding distance to the dephasing spin. The REDOR evolution time of 2.2 ms enables complete dephasing of carbons directly bonded to ¹⁵N. Standard REDOR for Figure 2 made use of alternating π -pulses on ¹³C and ¹⁵N channels with XY8 phase cycling and echo detection. For REDOR NMR, the decoupling field strengths were also 92 kHz (using TPPM) during acquisition and during periods containing REDOR pulses and employed ¹³C and ¹⁵N π -pulses of 10 µs.

Author Contributions

Sabrina H. Werby Conceptualization, Methodology, Investigation, Formal Analysis, Visualization, Writing. **Jasna Brcic** Investigation, Formal Analysis. **Madeline B. Chosy** Investigation. **Jiuzhi Sun** Investigation, Formal Analysis. **Jacob T. Rendell** Conceptualization, Resources. **Lewis F. Neville** Conceptualization, Resources. **Paul A. Wender** Conceptualization, Methodology, Formal Analysis, Writing, Funding Acquisition. **Lynette Cegelski** Conceptualization, Methodology, Formal Analysis, Visualization, Writing, Funding Acquisition.

Conflicts of interest

We note that Stanford University has filed patent applications on this and related technology, supported in part by the National Institutes of Health grants R01GM117278 (L.C.) and NIH-CA031845 and NSF CHE-1566423 (P.A.W.), which has been licensed by SuperTrans Medical for the treatment of bacterial infectious diseases.

Acknowledgements

This work was supported by the National Institutes of Health Grants R01GM117278 (L.C.) and NIH-CA031845 (P.A.W.), NSF CHE-1566423 (P.A.W.), and by SuperTrans Medical Ltd (Israel) (L.C. and P.A.W.). We acknowledge support through fellowships from the National Science Foundation Graduate Research Fellowship Program (NSF GRFP) (S.H.W.) and the Stanford Center for Molecular Analysis and Design (M.B.C. and J.S.) and through the Cystic Fibrosis Foundation Postdoctoral Fellowship (J.B.).

References

- World Health Organization. Global Priority List of Antibiotic-Resistant Bacteria to Guide Research, Discovery, and Development of New Antibiotics. Geneva: WHO Press 2017, 1–7.
- United Nations Interagency Coordination Group on Antimicrobial Resistance. No time to Wait: Securing the future from drug-resistant infections, 2019. <https://www.who.int/publications-detail-redirect/no-time-to-wait-securing-the-future-from-drug-resistant-infections>.
- Reynolds, P. E. Structure. *Eur. J. Clin. Microbiol. Infect. Dis.* 1989, **8** (11), 943–950.
- Walsh, C. T.; Fisher, S. L.; Park, I. S.; Prahalad, M.; Wu, Z. *Chem. Biol.* 1996, **3** (1), 21–28.
- Key reference: Antonoplis, A.; Zang, X.; Huttner, M. A.; Chong, K. K. L.; Lee, Y. B.; Co, J. Y.; Amieva, M. R.; Kline, K. A.; Wender, P. A.; Cegelski, L. *J. Am. Chem. Soc.* 2018, **140** (47), 16140–16151.
- Key reference: Stanzl, E. G.; Trantow, B. M.; Vargas, J. R.; Wender, P. A. *Acc. Chem. Res.* 2013, **46** (12), 2944–2954.
- Bechara, C.; Sagan, S. *FEBS Lett.* 2013, **587** (12), 1693–1702.
- Torchilin, V. P. *Adv. Drug Deliv. Rev.* 2008, **60** (4–5), 548–558.
- Nakase, I.; Takeuchi, T.; Futaki, S. *Methods Mol. Biol.* 2015, **1324**, 387–396.

- 10 Madani, F.; Lindberg, S.; Langel, U.; Futaki, S.; Gräslund, A. *J. Biophys.* 2011, **2011**, 414729.
- 11 Samuel, B. U.; Hearn, B.; Mack, D.; Wender, P.; Rothbard, J.; Kirisits, M. J.; Mui, E.; Wernimont, S.; Roberts, C. W.; Muench, S. P.; Rice, D. W.; Prigge, S. T.; Law, A. B.; McLeod, R. *Proc. Natl. Acad. Sci. U S A* 2003, **100** (24), 14281–14286.
- 12 Sparr, C.; Purkayastha, N.; Kolesinska, B.; Gengenbacher, M.; Amulic, B.; Matuschewski, K.; Seebach, D.; Kamena, F. *Antimicrob. Agents Chemother.* 2013, **57** (10), 4689–4698.
- 13 Lei, E. K.; Pereira, M. P.; Kelley, S. O. *Angew. Chem. Int. Ed. Engl.* 2013, **52** (37), 9660–9663.
- 14 Purkayastha, N.; Capone, S.; Beck, A. K.; Seebach, D.; Leeds, J.; Thompson, K.; Moser, H. E. *Chem. Biodivers.* 2015, **12** (2), 179–193.
- 15 Luedtke, N. W.; Carmichael, P.; Tor, Y. *J. Am. Chem. Soc.* 2003, **125** (41), 12374–12375.
- 16 Dubikovskaya, E. A.; Thorne, S. H.; Pillow, T. H.; Contag, C. H.; Wender, P. A. *Proc. Natl. Acad. Sci. U S A* 2008, **105** (34), 12128–12133.
- 17 Wender, P. A.; Galliher, W. C.; Bhat, N. M.; Pillow, T. H.; Bieber, M. M.; Teng, N. N. *H. Gynecol. Oncol.* 2012, **126** (1), 118–123.
- 18 Rothbard, J. B.; Garlington, S.; Lin, Q.; Kirschberg, T.; Kreider, E.; McGrane, P. L.; Wender, P. A.; Khavari, P. A. *Nat. Med.* 2000, **6** (11), 1253–1257
- 19 Chen, L.; Wright, L. R.; Chen, C. H.; Oliver, S. F.; Wender, P. A.; Mochly-Rosen, D. *Chem. Biol.* 2001, **8** (12), 1123–1129.
- 20 Jameson, K. L.; Mazur, P. K.; Zehnder, A. M.; Zhang, J.; Zarnegar, B.; Sage, J.; Khavari, P. A. *Nat. Med.* 2013, **19** (5), 626–630.
- 21 Benner, N. L.; Zang, X.; Buehler, D. C.; Kickhoefer, V. A.; Rome, M. E.; Rome, L. H.; Wender, P. A. *ACS Nano* 2017, **11** (1), 872–881.
- 22 Hyman, J. M.; Geihe, E. I.; Trantow, B. M.; Parvin, B.; Wender, P. A. *Proc. Natl. Acad. Sci. U S A* 2012, **109** (33), 13225–13230.
- 23 Pavlovic, I.; Thakor, D. T.; Vargas, J. R.; McKinlay, C. J.; Hauke, S.; Anstaett, P.; Camuña, R. C.; Bigler, L.; Gasser, G.; Schultz, C.; Wender, P. A.; Jessen, H. J. *Nat. Commun.* 2016, **7**, 10622.
- 24 Geihe, E. I.; Cooley, C. B.; Simon, J. R.; Kiesewetter, M. K.; Edward, J. A.; Hickerson, R. P.; Kaspar, R. L.; Hedrick, J. L.; Waymouth, R. M.; Wender, P. A. *Proc. Natl. Acad. Sci. U S A* 2012, **109** (33), 13171–13176.
- 25 Wender, P. A.; Huttner, M. A.; Staveness, D.; Vargas, J. R.; Xu, A. F. *Mol. Pharm.* 2015, **12** (3), 742–750.
- 26 Siprashvili, Z.; Scholl, F. A.; Oliver, S. F.; Adams, A.; Contag, C. H.; Wender, P. A.; Khavari, P. A. *Hum. Gene. Ther.* 2003, **14** (13), 1225–1233.
- 27 Key reference: Antonoplis, A.; Zang, X.; Wegner, T.; Wender, P. A.; Cegelski, L. *ACS Chem Biol* 2019, **14** (9), 2065–2070.
- 28 Key reference: Neville, L. F.; Shalit, I.; Warn, P. A.; Scheetz, M. H.; Sun, J.; Chosy, M. B.; Wender, P. A.; Cegelski, L.; Rendell, J. T. *Antimicrob. Agents Chemother.* 2021, **65** (4), e02416-20.
- 29 Key reference: Neville, L. F.; Shalit, I.; Warn, P. A.; Rendell, J. T. *J. Antimicrob. Chemother.* 2022, **77**(6), 1706-9.
- 30 Sarkar, P.; Samaddar, S.; Ammanathan, V.; Yarlagadda, V.; Ghosh, C.; Shukla, M.; Kaul, G.; Manjithaya, R.; Chopra, S.; Haldar, J. *ACS Chem Biol* 2020, **15** (4), 884–889.
- 31 Wu, Z.-C.; Cameron, M. D.; Boger, D. L. *ACS Infect. Dis.* 2020, **6** (8), 2169–2180.
- 32 Wu, Z.-C.; Isley, N. A.; Okano, A.; Weiss, W. J.; Boger, D. L. *J. Org. Chem.* 2020, **85** (3), 1365–1375.
- 33 Wu, Z.-C.; Boger, D. L. *Tetrahedron* 2019, **75** (24), 3160–3165.
- 34 Umstätter, F.; Domhan, C.; Hertlein, T.; Ohlsen, K.; Mühlberg, E.; Kleist, C.; Zimmermann, S.; Beijer, B.; Klika, K. D.; Haberkorn, U.; Mier, W.; Uhl, P. *Angew. Chem. Int. Ed. Engl.* 2020, **59** (23), 8823–8827.
- 35 Blaskovich, M. A. T.; Hansford, K. A.; Gong, Y.; Butler, M. S.; Muldoon, C.; Huang, J. X.; Ramu, S.; Silva, A. B.; Cheng, M.; Kavanagh, A. M.; Ziora, Z.; Premraj, R.; Lindahl, F.; Bradford, T. A.; Lee, J. C.; Karoli, T.; Pelington, R.; Edwards, D. J.; Amado, M.; Elliott, A. G.; Phetsang, W.; Daud, N. H.; Deecke, J. E.; Sidjabat, H. E.; Ramaologa, S.; Zuegg, J.; Betley, J. R.; Beevers, A. P. G.; Smith, R. A. G.; Roberts, J. A.; Paterson, D. L.; Cooper, M. A. *Nat. Commun.* 2018, **9** (1), 22.
- 36 Cheng, A. V.; Wuest, W. M. *ACS Infect. Dis.* 2019, **5** (6), 816–828.
- 37 Najjar, A.; Karaman, R. *Expert. Opin. Drug. Deliv.* 2019, **16** (1), 1–5.
- 38 Sloane, J. L.; Benner, N. L.; Keenan, K. N.; Zang, X.; Soliman, M. S. A.; Wu, X.; Dimapasoc, M.; Chun, T.-W.; Marsden, M. D.; Zack, J. A.; Wender, P. A. *Proc. Natl. Acad. Sci. U S A* 2020, **117** (20), 10688–10698.
- 39 Freije, I.; Lamouche, S.; Tanguay, M. *Ther. Innov. Regul. Sci.* 2020, **54** (1), 128–138.
- 40 Vermassen, A.; Leroy, S.; Talon, R.; Provot, C.; Popowska, M.; Desvaux, M. *Front. Microbiol.* 2019, **10**, 331.
- 41 Werby, S. H.; Cegelski, L. *J. Struct. Biol.* 2019, **206** (1), 49–54.
- 42 Nygaard, R.; Romaniuk, J. A. H.; Rice, D. M.; Cegelski, L. *Biophys. J.* 2015, **108** (6), 1380–1389.
- 43 Romaniuk, J. A. H.; Cegelski, L. *Biochem.* 2018, **57** (26), 3966–3975.
- 44 Romaniuk, J. A. H.; Cegelski, L. *Philos. Trans. R. Soc. Lond. B Biol. Sci.* 2015, **370** (1679), 20150024.
- 45 Cegelski, L.; Kim, S. J.; Hing, A. W.; Studelska, D. R.; O'Connor, R. D.; Mehta, A. K.; Schaefer, J. *Biochem.* 2002, **41**(43), 13053-13058.
- 46 Kim, S. J.; Cegelski, L.; Studelska, D. R.; O'Connor, R. D.; Mehta, A. K.; Schaefer, J. *Biochemistry* 2002, **41** (22), 6967–6977.
- 47 Cegelski, L.; Steuber, D.; Mehta, A. K.; Kulp, D. W.; Axelsen, P. H.; Schaefer, J. *J. Mol. Biol.* 2006, **357** (4), 1253–1262.
- 48 Kim, S. J.; Cegelski, L.; Preobrazhenskaya, M.; Schaefer, J. *Biochem.* 2006, **45**(16), 5235–5250.
- 49 Kim, S.J.; Cegelski, L.; Stueber, D.; Singh, M.; Dietrich, E.; Tanaka, K.S.; Parr Jr, T.R.; Far, A.R.; Schaefer, J. *J. Molec. Biol.* 2008, **377**(1), 281-293.
- 50 Mehta, A. K.; Cegelski, L.; O'Connor, R. D.; Schaefer, J. *J. Magn. Reson.* 2003, **163**(1), 182-187.
- 51 Singh, M.; Chang, J.; Coffman, L.; Kim, S. J. *Scient. Rep.* 2016, **6**(1), 31757.
- 52 Patti, G.J.; Kim, S.J.; Yu, T.Y.; Dietrich, E.; Tanaka, K.S.; Parr Jr, T.R.; Far, A.R.; Schaefer, J. *J. Molec. Biol.* 2009, **392**(5), pp.1178-1191.
- 53 Kim, S.J.; Matsuoka, S.; Patti, G.J.; Schaefer, J. *Biochem.* 2008, **47**(12), pp.3822-3831.
- 54 Kim, S. J.; Schaefer, J. *Biochemistry*, 2008, **47**(38), 10155-10161.
- 55 Kim, S.J.; Singh, M.; Sharif, S.; Schaefer, J. *Biochem.* 2017, **56**(10), pp.1529-1535.
- 56 Tardy-Laporte, C.; Arnold, A.A.; Genard, B.; Gastineau, R.; Moranças, M.; Mouget, J.L.; Tremblay, R.; Marcotte, I. *Biochim. Biophys. Acta-Biomem.* 2013, **1828**(2), pp.614-622.
- 57 Overall, S. A.; Zhu, S.; Hanssen, E.; Separovic, F.; Sani, M. A. *Int. J. Mol. Sci.* 2019, **20**(1), 181.
- 58 Separovic, F.; Hofferek, V.; Duff, A. P.; McConville, M. J.; Sani, M. A. *J. Struct. Biol.*: X, 2022, **6**, 100074.
- 59 Udekwu, K. I.; Parrish, N.; Ankomah, P.; Baquero, F.; Levin, B. R. *J. Antimicrob. Chemother.* 2009, **63** (4), 745–757.
- 60 Schaefer, J.; Stejskal, E. O. *J. Am. Chem. Soc.* 1976, **98** (4), 1031–1032.
- 61 Gullion, T.; Schaefer, J. *J. Magn. Reson.* 1989, **81** (1), 196–200.
- 62 Nygaard, R.; Romaniuk, J. A.; Rice, D. M.; Cegelski, L. *J. Phys. Chem. B* 2017, **121**(40), 9331-9335.
- 63 Morcombe, C. R.; Zilm, K. W. *J. Magn. Reson.* 2003, **162**,479-486.